Discrete Spatial Optical Solitons in Waveguide Arrays

H. S. Eisenberg and Y. Silberberg
Department of Physics of Complex Systems, Weizmann Institute of Science, Rehovot 76100, Israel

R. Morandotti, A. R. Boyd, and J. S. Aitchison
Department of Electronics and Electrical Engineering, University of Glasgow, Glasgow G12 8QQ, Scotland
(Received 25 June 1998)

We report the observation of discrete spatial optical solitons in an array of 41 waveguides. Light was coupled to the central waveguide. At low power, the propagating field spreads as it couples to more waveguides. When sufficient power was injected, the field was localized close to the input waveguides and its distribution was successfully described by the discrete nonlinear Schrödinger equation. [S0031-9007(98)07295-0]

PACS numbers: 42.65.Tg, 03.40.Kf, 42.65.Wi, 42.82.Et

In the early days of nonlinear optics it was proposed [1] that light beams can trap themselves by creating their own waveguide through the nonlinear Kerr effect. The connection between self-trapping and soliton theory was first made by Zakharov and Shabat [2], who showed that there are two kinds of optical solitons, spatial and temporal, where the nonlinear effect balances diffraction and dispersion, respectively. For spatial solitons to exist in Kerr media, diffraction has to be confined to one transverse dimension. Experimental demonstrations in planar waveguides, where the other transverse dimension is confined by the waveguide, have been reported [3]. Such solitons are solutions of the nonlinear Schrödinger equation which represents one type of partial differential equation with solitary solutions.

It has been proposed that a phenomenon similar to that of spatial solitons should occur in an infinite array of identical, weakly coupled waveguides [4,5]. In such an array, when low intensity light is injected into one, or a few neighboring waveguides, it will couple to more and more waveguides as it propagates, thereby broadening its spatial distribution. This widening distribution is analogous to diffraction in continuous media. A high intensity changes the refractive index of the input waveguides through the Kerr effect and decouples them from the rest of the array. It has been shown that certain light distributions propagate while keeping a fixed spatial profile among a limited number of waveguides, in an analogous way to spatial solitons; these are *discrete spatial solitons*.

Let us consider an infinite array of one dimensional identical waveguides. They are positioned with equal separations D between each other such that all the coupling constants between them are equal. The equation which describes the evolution of E_n, the electrical field in the nth waveguide, in the presence of the optical Kerr effect, is

$$i\,\frac{dE_n}{dz} + \beta E_n + C(E_{n-1} + E_{n+1}) + \gamma|E_n|^2 E_n = 0\,, \tag{1}$$

where β is the linear propagation constant, C is the coupling constant, $\gamma = \frac{\omega_0 n_2}{cA_{\text{eff}}}$, ω_0 is the optical angular frequency, n_2 is the nonlinear coefficient, and A_{eff} is the common effective area of the waveguide modes. This equation is sometimes referred to as the discrete nonlinear Schrödinger equation (DNLSE). At low powers, the nonlinear term of Eq. (1) can be ignored. The infinite set of ordinary differential equations is then analytically integrable [6]. The solution for the nth waveguide, when only one waveguide is excited, is a set of Bessel functions. If we set $E_0 = A_0$ and $E_{n\neq 0} = 0$ at $z = 0$, the solution for the electrical field in the nth waveguide is

$$E_n(z) = A_0(i)^n \exp(i\beta z) J_n(2Cz)\,, \tag{2}$$

where $J_n(x)$ is a Bessel function of order n. This distribution is displayed in Fig. 1. As the light propagates along the waveguides, the energy spreads into two main lobes with several secondary peaks between them. The solution under any other initial conditions will be a linear superposition of Eq. (2).

When the intensity varies slowly over adjacent waveguides, the discrete set of ordinary differential equations [Eq. (1)] can be reduced to the nonlinear Schrödinger equation which describes spatial solitons [4]. It has been shown numerically [4,5] that at high enough power, introducing a field distribution to the array such as $E_n(z) = A_0 \exp[i(2C + \beta)z]\,\text{sech}[\frac{X_n}{X_0}]$, where X_n is the location of the nth waveguide and X_0 is the characteristic width, will result in a localized propagating distribution.

Numerical simulations show that these localized distributions share a few basic properties with solitons and differ in a few others [5]. For example, just like spatial solitons, discrete solitons do not have to propagate in the direction of the waveguides. When a discrete soliton is launched with a linear phase gradient across the waveguides, it will propagate at an angle to the direction of the waveguides. However, as the soliton power is increased, it may change its direction of propagation [5]. It

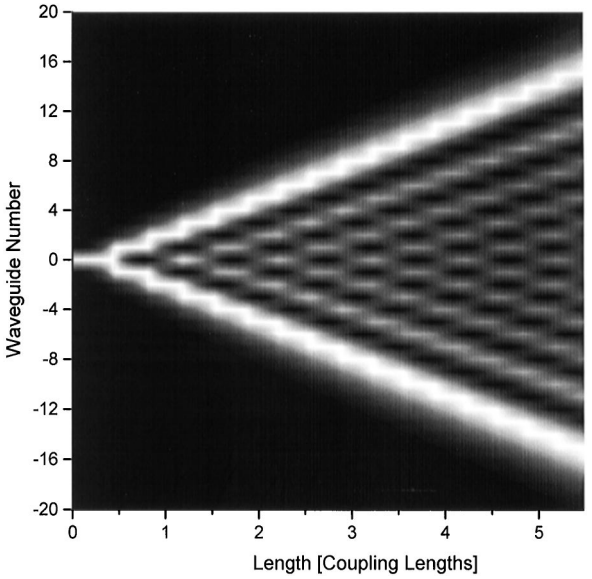

FIG. 1. Solution for a linearly coupled array of 41 waveguides, when light is injected into the central waveguide, with $E_0 = 1$. The intensity is shown in gray scale. The scale is chosen such that the peak intensity for every propagation distance along the waveguide is represented by white. The energy is spread mainly into two lobes. The number of central peaks is an indication to how many coupling lengths the light has propagated.

has been shown that the location of the center of the soliton, whether centered on a waveguide or in between two waveguides, has an effect on the stability of the soliton to small tilts of the phase. Briefly, a soliton centered in between waveguides is easier to steer than a soliton centered on a guide [7,8].

The DNLSE [Eq. (1)] and its localized propagating modes appear in several other fields. This equation describes, for example, localized modes in molecular systems such as long proteins [9], polarons in one dimensional ionic crystals [10], localized modes in electrical lattices [11], and a coupled array of nonlinear mechanical pendulums [12]. These localized modes are an example of the more general phenomenon of *discrete breathers* [13] to which discrete solitons belong. A few other realizations are reviewed in Ref. [13].

In our experiments we studied arrays of 41 ridge waveguides etched onto an AlGaAs substrate [14]. A section of the sample is illustrated in the inset of Fig. 2. The waveguides, each 4 μm wide, are etched on top of a slab waveguide. The etching depth is 0.95 μm. Samples with different separation parameters were studied. The separation D affects the coupling coefficient C in Eq. (1). In our samples, $D = 4$, 5, and 7 μm. The mode effective area is about 19 μm^2 and its ellipticity ratio is about 2.5:1.

Our light source was an optical parametric oscillator (OPO) pumped by a Ti:sapphire laser, producing 100–200 fs pulses at a 80 MHz repetition rate. The OPO was tuned to a wavelength of 1.53 μm, which is below the half-band-gap of the AlGaAs material and where detrimental effects of nonlinear absorption are minimized. The setup is sketched in Fig. 2. The injected power was controlled by a variable filter and sampled into an input detector. The polarization was controlled by a half-wave plate and a polarizer. The beam was reshaped by a cylindric telescope into an oval shape in order to match the waveguide mode. The light was coupled into one facet of the sample through a $\times 40$ objective and collected

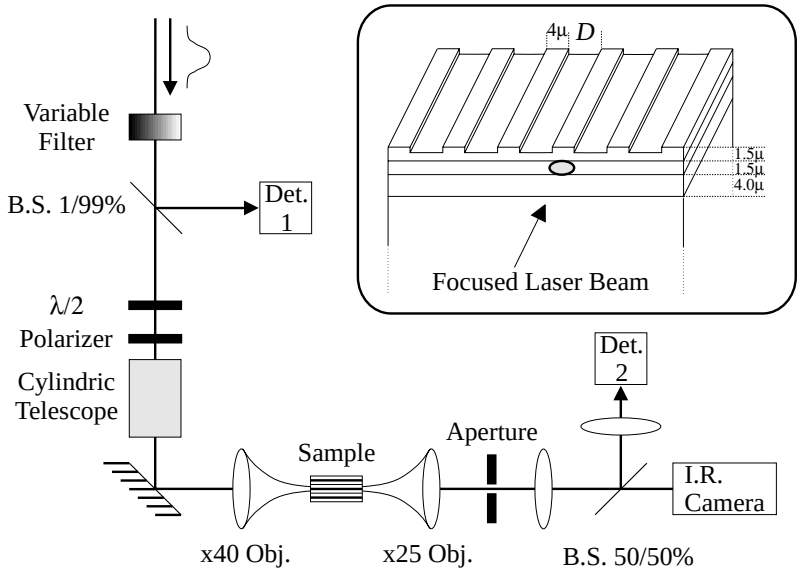

FIG. 2. The experimental setup. Inset: Schematic drawing of the sample. The sample consists of a $Al_{0.18}Ga_{0.82}As$ core layer and $Al_{0.24}Ga_{0.76}As$ cladding layers grown on top of a GaAs substrate. A few samples were tested with different separations D between the waveguides.

with a $\times 25$ objective at the output side. The sample was mounted on a piezoelectric driven xyz stage and imaged from above onto a CCD camera in order to aid the alignment process. The output facet was imaged onto an infrared camera. Half the power was focused into an output detector in order to measure the output power.

We first present data taken from a 6 mm long array with waveguide separation $D = 4\ \mu$m, which is relatively strongly coupled. The output facet images at various input powers are shown in Fig. 3. At low power, linear behavior is demonstrated. The light spreads among nearly all the 41 waveguides, and a pattern of two main lobes with secondary peaks between them is formed. From this pattern we conclude that the sample is about four coupling lengths long, as we match it to the distribution in Fig. 1. Increasing the power narrows the light distribution until a discrete spatial soliton is formed. Numerical simulations verify that although light was coupled into a single waveguide, light is distributed within one coupling length over a few waveguides. From there on, the distribution remains confined, with only small width oscillations around the soliton value.

We also investigated 6 mm long samples with weaker coupling, with waveguide separations of 5 and 7 μm. TM and TE polarized light, respectively, at low and high powers, was injected into these samples. The respective high intensity peak powers were estimated to be 960 and 870 W. The measured output patterns at low and high intensities are shown in Figs. 4 and 5.

Also shown in the figures are numerical predictions for the intensity distribution among the waveguides, depicted as vertical lines in the figures. These theoretical lines were obtained by integrating the DNLSE for the 41 waveguides, using a fifth order adaptive step size Runge-Kutta algorithm. The linear parameters were obtained from the low power measurements. The nonlinear coefficient was then adjusted to match the high power results.

We found that the sample lengths, in units of coupling length, were 3.0 and 1.9 for the $D = 5\ \mu$m and $D = 7\ \mu$m samples, respectively. The parameter C was calculated to be 0.82 (0.52) mm^{-1} for the 5 (7) μm separation sample. The value of γ was calculated from the waveguide parameters to be 3.6 m^{-1} W^{-1} for TE polarization and 3.35 m^{-1} W^{-1} for TM polarization. The value of γ that best fits the high power results for the 5 (7) μm sample for TM (TE) is 5.4 (6.2) m^{-1} W^{-1}.

The agreement between the experimental results and the theory is quite satisfactory, even though Eq. (1) assumes cw propagation, while the experiments were performed with a pulsed source. This fact does not affect the linear propagation, but we should expect an effect at high powers. There are two sources for error: the intensity varies along the temporal profile; hence we expect the peak of the pulse to exhibit more confinement than its temporal wings. In addition, dispersion broadens the pulse by almost a factor of 2 as it propagates along the array, thereby reducing the peak power. These differences probably explain why the experimental field distributions are slightly broader than the cw theory prediction. They

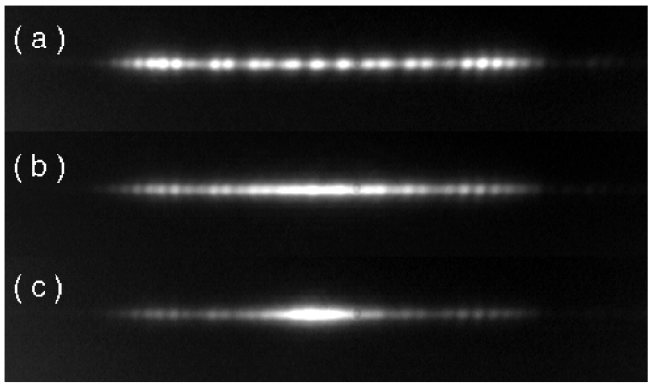

FIG. 3. Images of the output facet of a sample with $D = 4\ \mu$m for different powers. (a) Peak power 70 W. Linear features are demonstrated: two main lobes and a few secondary peaks in between. (b) Peak power 320 W. Intermediate power, the distribution is narrowing. (c) Peak power 500 W. A discrete soliton is formed.

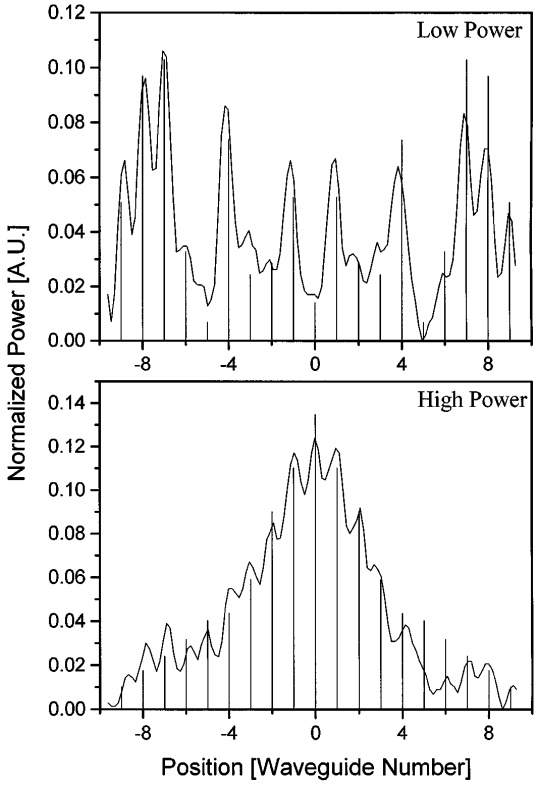

FIG. 4. Experimental and numerical results for a sample with $D = 5\ \mu$m. Experimental results are represented by a solid curve and numerical results are shown as vertical lines. The total propagation distance is 3.0 coupling lengths. The integrated power is normalized to unity.

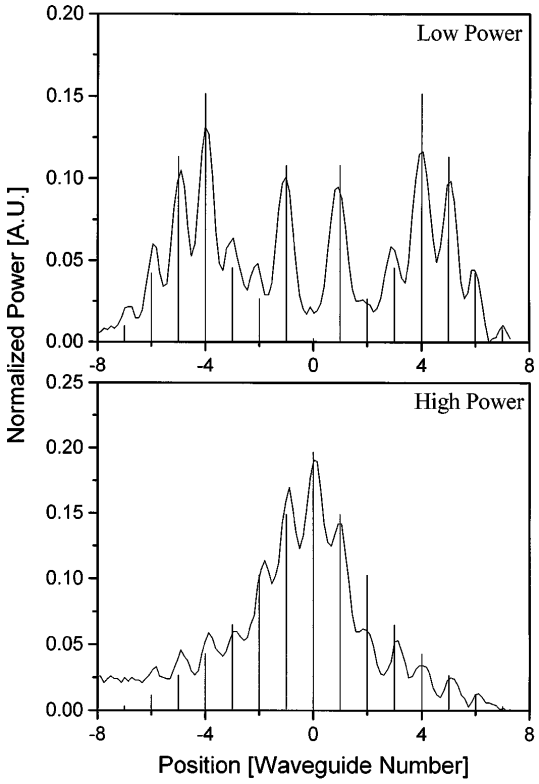

FIG. 5. As in Fig. 4, with $D = 7\ \mu$m. The total propagation distance is 1.9 coupling lengths.

also explain the side wings emerging at high energy (Fig. 4).

In conclusion, we have studied the formation of discrete spatial solitons in nonlinear waveguide arrays made of AlGaAs below the half-band-gap. We have shown a power dependent localization of the output distribution. We have also found preliminary evidence for power dependent discrete soliton steering and for the existence and stability of the two types of confined modes [5,7], which will be reported separately later.

This work was supported in part by the UK-Israel Science and Technology Research Fund and the Israeli Ministry of Science.

[1] R. Y. Chiao, E. Garmire, and C. H. Townes, Phys. Rev. Lett. **13**, 479 (1964).
[2] V. E. Zakharov and A. B. Shabat, Zh. Eksp. Teor. Fiz. **61**, 118 (1971) [Sov. Phys. JETP **34**, 62 (1972)].
[3] A. Barthelemy, S. Maneuf, and C. Froehly, Opt. Commun. **55**, 201 (1985); J. S. Aitchison, Y. Silberberg, A. M. Weiner, D. E. Leaird, M. K. Oliver, J. L. Jackel, E. M. Vogel, and P. W. E. Smith, J. Opt. Soc. Am. B **8**, 1290 (1990); J. S. Aitchison, K. Al-Hemyari, C. N. Ironside, R. S. Grant, and W. Sibbett, Electron. Lett. **28**, 1879 (1992).
[4] D. N. Christodoulides and R. I. Joseph, Opt. Lett. **13**, 794 (1988).
[5] A. B. Aceves, C. De Angelis, T. Peschel, R. Muschall, F. Lederer, S. Trillo, and S. Wabnitz, Phys. Rev. E **53**, 1172 (1996).
[6] A. Yariv, *Optical Electronics* (Saunders College Publishing, Philadelphia, 1991), 4th ed., pp. 519–524.
[7] W. Królikowski and Y. Kivshar, J. Opt. Soc. Am. B **13**, 876 (1996).
[8] Y. S. Kivshar and D. K. Campbell, Phys. Rev. E **48**, 3077 (1993).
[9] A. S. Davydov, Phys. Scr. **20**, 387 (1978).
[10] T. Holstein, Ann. Phys. (N.Y.) **8**, 325 (1959); Mol. Cryst. Liq. Cryst. **77**, 235 (1981).
[11] P. Marquié, J. M. Bilbault, and M. Remoissenet, Phys. Rev. E **51**, 6127 (1995).
[12] B. Denardo, B. Galvin, A. Greenfield, A. Larraza, S. Putterman, and W. Wright, Phys. Rev. Lett. **68**, 1730 (1992).
[13] S. Flach and C. R. Willis, Phys. Rep. **295**, 182 (1998).
[14] P. Millar, J. S. Aitchison, J. U. Kang, G. I. Stegeman, A. Villeneuve, G. T. Kennedy, and W. Sibbett, J. Opt. Soc. Am. B **14**, 3224 (1997).